ELSEVIER

Thermochimica Acta 313 (1998) 201–206

thermochimica
acta

The heat capacity of $Y_3Al_5O_{12}$ from 0 to 900 K

R.J.M. Konings[a,*], R.R. van der Laan[a], A.C.G. van Genderen[b], J.C. van Miltenburg[b]

[a] *Netherlands Energy Research Foundation ECN, P.O. Box 1, 1755 ZG Petten, The Netherlands*
[b] *Thermodynamic Centre, Utrecht University, Padualaan 8, 3584 CH, Utrecht, The Netherlands*

Received 3 December 1997; received in revised form 9 January 1998; accepted 11 January 1998

Abstract

The heat capacity of yttrium aluminium garnet $Y_3Al_5O_{12}$ (YAG) has been measured by low-temperature adiabatic calorimetry from 5 to 420 K. For temperatures up to 900 K the heat capacity has been derived from enthalpy-increment measurements (470–880 K) using high-temperature drop calorimetry. The two sets of calorimetric data join smoothly and show no transition in the measured temperature range. © 1998 Elsevier Science B.V.

Keywords: Yttrium aluminium garnet; Heat capacity; Entropy; Calorimetry; Thermodynamic properties

1. Introduction

Yttrium aluminium garnet $Y_3Al_5O_{12}$ (YAG), widely known for its application in lasers, has been suggested as high-temperature ceramic for use as support material in uranium-free nuclear fuels for the transmutation of actinides (e.g. plutonium or americium) [1]. From the point of view of neutronics, YAG has favourable properties since its constituting elements (O, Al, Y) have relatively small cross-sections for neutron capture. Other properties of YAG that need to be known to judge its applicability as support material in uranium-free fuels are (i) its radiation stability towards neutrons, alpha decay (α-particles and recoil atoms), and fission product particles, and (ii) its thermal and mechanical behaviour. Both items are being studied in our current research programme on uranium-free fuels [2].

Surprisingly, experimental data for the thermal properties of YAG are scarce. In a literature survey, we found a limited number of high-temperature studies performed by Soviet scientists (see [3] and references therein). However, these were published in difficult accessible sources and are not available to us. To our knowledge, low-temperature measurements have not been performed. Therefore, we have measured the heat capacity of YAG in the low-temperature as well as the high-temperature range, the results of which are reported in the present paper.

2. Experimental

The YAG sample was purchased from Cerac (lot number 87513-A-1). It was specified to be 99.9% pure (impurities Ca<0.01%, Cu<0.01%, Fe 0.02%, Mg<0.01%, Si 0.01%). Before use the sample was heated at 573 K in purified argon. X-ray diffraction analysis showed only the presence of cubic YAG.

---

*Corresponding author. Fax: 0031224563608; e-mail: konings@ecn.nl

PII S0040-6031(98)00261-5

The low-temperature calorimetric measurements were performed at the Utrecht University, using the adiabatic calorimeter CAL V. Details of the equipment have been described in [4]. The weight of the sample for the low-temperature measurements was 10.368 g.

The enthalpy increments were measured in an isothermal diphenyl-ether drop calorimeter, as previously described in [5]. For the experiment 5.33371 g of YAG was enclosed in a quartz capsule of 1.37627 g.

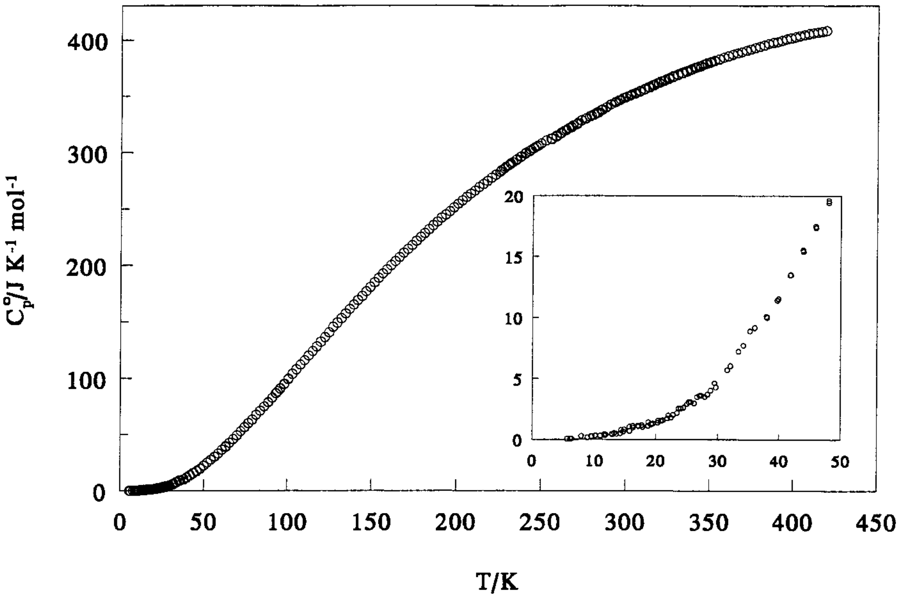

Fig. 1. Experimental heat capacity curve of YAG.

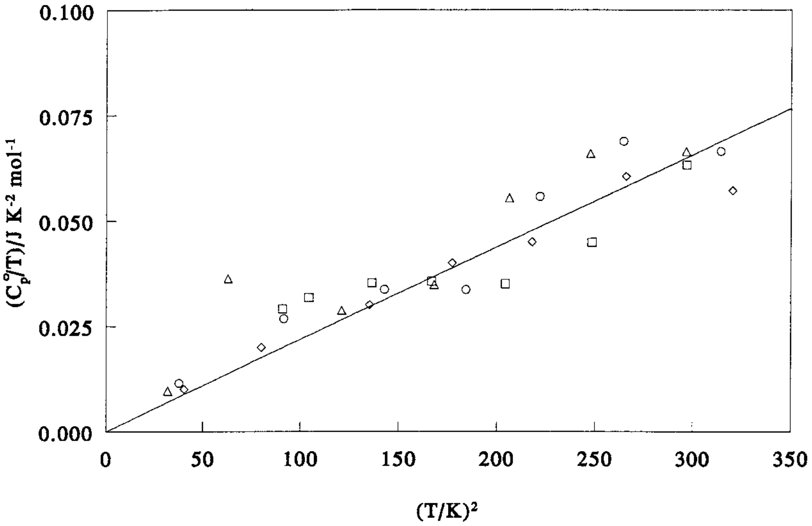

Fig. 2. Low-temperature heat capacity of YAG; □, run 3; ○, run 4; △, run 6; ◇, run 7.

Table 1
The low-temperature heat capacity data for YAG

T (K)	C_p^0 (J·K^{-1}·mol^{-1})	T (K)	C_p^0 (J·K^{-1}·mol^{-1})	T (K)	C_p^0 (J·K^{-1}·mol^{-1})	T (K)	C_p^0 (J·K^{-1}·mol^{-1})
run 2							
226.23	284.4	279.03	332.7	330.16	368.9	379.20	394.1
228.69	287.0	281.95	335.1	332.94	370.5	381.88	395.4
231.67	290.3	284.86	337.5	335.70	372.0	384.56	396.7
234.64	293.2	287.76	339.9	338.47	373.7	387.23	397.6
237.60	296.1	290.65	342.5	341.22	375.4	389.91	398.3
240.56	299.6	293.52	344.6	343.97	376.5	392.57	399.5
243.52	302.4	296.39	346.9	346.71	378.6	395.24	400.7
246.48	305.3	299.25	348.8	349.44	379.8	397.90	401.7
249.44	308.2	302.10	350.7	352.17	381.4	400.56	402.7
252.41	310.8	304.94	352.3	354.89	382.8	403.22	403.8
255.37	312.4	307.77	354.2	357.61	384.3	405.87	404.6
258.34	314.3	310.60	356.2	360.33	385.6	408.52	405.4
261.31	317.3	313.41	358.1	363.04	386.9	411.18	406.1
264.28	320.0	316.22	360.0	365.74	388.2	413.82	406.7
267.24	322.5	319.02	361.9	368.44	389.4	416.47	407.5
270.20	325.1	321.82	363.6	371.14	390.6	419.11	408.2
273.16	328.3	324.61	365.6	373.83	391.8		
276.10	330.4	327.39	367.2	376.52	393.0		
run 3							
9.54	0.277	14.29	0.501	20.31	1.37	26.62	3.53
10.21	0.325	15.76	0.707	21.85	1.73	28.30	3.73
11.68	0.412	17.23	1.09	23.42	2.20		
12.91	0.460	18.78	1.12	25.00	2.95		
run 4							
6.15	0.071	14.89	0.831	20.86	1.53	27.27	3.64
9.57	0.256	16.26	1.12	22.43	1.80		
11.95	0.403	17.73	1.18	24.02	2.58		
13.57	0.457	19.22	1.25	25.62	3.09		
run 5							
29.47	4.665	47.98	19.46	67.67	45.97	88.57	78.79
32.02	6.062	50.08	22.13	69.95	49.39	90.94	82.95
34.13	7.756	52.20	25.03	72.24	53.10	93.31	86.94
36.01	9.190	54.35	27.62	74.54	56.54	95.69	90.95
37.91	10.10	56.52	30.32	76.85	60.06	98.07	94.83
39.87	11.57	58.72	33.21	79.18	63.13	100.45	99.17
41.86	13.53	60.93	36.52	81.51	67.52		
43.87	15.43	63.16	39.68	83.86	71.25		
45.91	17.37	65.41	42.81	86.21	75.06		
run 6							
5.65	0.0546	14.36	0.7966	20.38	1.570	27.04	3.641
7.93	0.2877	15.73	1.038	21.99	1.991	28.81	4.061
11.00	0.3160	17.22	1.145	23.63	2.580		
12.96	0.4508	18.79	1.414	25.31	3.109		
run 7							
6.36	0.0640	16.30	0.9872	24.45	2.641	33.33	7.266
8.95	0.1790	17.90	1.024	26.14	3.002	35.19	8.911
11.63	0.3500	19.52	1.315	27.89	3.524		
13.31	0.5320	21.12	1.589	29.69	4.310		
14.76	0.6640	22.77	2.048	31.51	5.709		

Table 1
(continued)

T (K)	C_p^0 (J·K^{-1}·mol^{-1})	T (K)	C_p^0 (J·K^{-1}·mol^{-1})	T (K)	C_p^0 (J·K^{-1}·mol^{-1})	T (K)	C_p^0 (J·K^{-1}·mol^{-1})
run 8							
38.04	10.01	52.20	25.10	67.69	46.03	83.89	71.34
39.69	11.44	54.36	27.61	69.97	49.46	86.25	75.14
41.79	13.50	56.54	30.19	72.27	53.06	88.61	78.98
43.82	15.56	58.73	33.17	74.57	56.66	90.98	83.03
45.87	17.49	60.95	36.62	76.89	60.07		
47.96	19.61	63.18	39.71	79.21	63.26		
50.07	22.30	65.43	42.84	81.55	67.69		
run 9							
93.04	86.88	131.99	153.1	173.56	218.0	215.49	272.2
94.07	88.46	134.43	157.4	176.03	221.7	217.96	274.9
95.79	91.18	136.86	161.3	178.49	225.3	220.44	277.7
98.21	95.08	139.30	165.2	180.95	228.6	222.92	280.3
100.60	99.51	141.75	169.2	183.41	232.0	225.39	283.0
102.99	103.9	144.19	172.8	185.88	235.3	227.87	285.9
105.38	107.9	146.62	176.9	188.34	238.6	230.34	288.6
107.78	112.1	149.06	180.8	190.81	242.1	232.82	291.3
110.19	116.0	151.51	184.9	193.27	244.8	235.29	293.9
112.60	120.2	153.95	188.9	195.74	247.8	237.77	296.5
115.01	124.2	156.40	192.7	198.20	251.3	240.25	298.9
117.43	128.3	158.85	196.3	200.67	254.5	242.74	301.2
119.85	132.4	161.30	200.1	203.14	257.5	245.22	303.9
122.27	136.4	163.75	203.7	205.61	260.5	247.70	306.2
124.70	140.6	166.20	207.4	208.08	263.6		
127.12	145.4	168.65	211.1	210.55	266.3		
129.56	149.2	171.11	214.6	213.02	269.3		
run 10							
255.78	312.0	280.54	333.5	305.38	353.2	330.24	369.3
258.25	314.9	283.02	335.1	307.86	354.7	332.73	370.8
260.73	317.3	285.52	337.8	310.35	356.5	335.22	372.3
263.20	319.3	288.02	340.1	312.83	358.2	337.71	373.7
265.67	321.7	290.49	342.5	315.32	359.9	340.21	375.2
268.14	324.0	292.97	344.5	317.80	361.5	342.70	376.5
270.61	326.1	295.45	346.3	320.29	363.1	345.19	378.0
273.09	328.5	297.93	348.3	322.78	364.6	347.68	379.3
275.57	330.1	300.41	349.9	325.26	366.2	350.18	380.6
278.05	332.0	302.89	351.6	327.75	367.9		

3. Results and discussion

The low-temperature heat capacity measurements were performed in 10 runs, which are highly reproducible with the exception of run 1. The C_p values obtained in run 1 are somewhat lower than those of the subsequent runs and therefore these data have been excluded. The results for run 2 to 10 are listed in Table 1 and shown in Fig. 1. The heat capacity increases smoothly from 0 to 420 K, showing no anomalies.

The experimental data up to 18 K have been fitted to the function $C_p^0 = \alpha T^3$, yielding $\alpha = 0.219\times10^{-3}$ J·K^{-4}·mol^{-1} (Fig. 2). At 10 K, we then obtain $C_p^0 = 0.219$ J·K^{-1}·mol^{-1}, and, by integration from 0 K, S^0 (10 K) $= 0.073$ J·K^{-1}·mol^{-1} and H^0(10 K)$-H^0$(0 K) $= 0.547$ J·mol^{-1}. These values have been used as starting values for the calculation of the

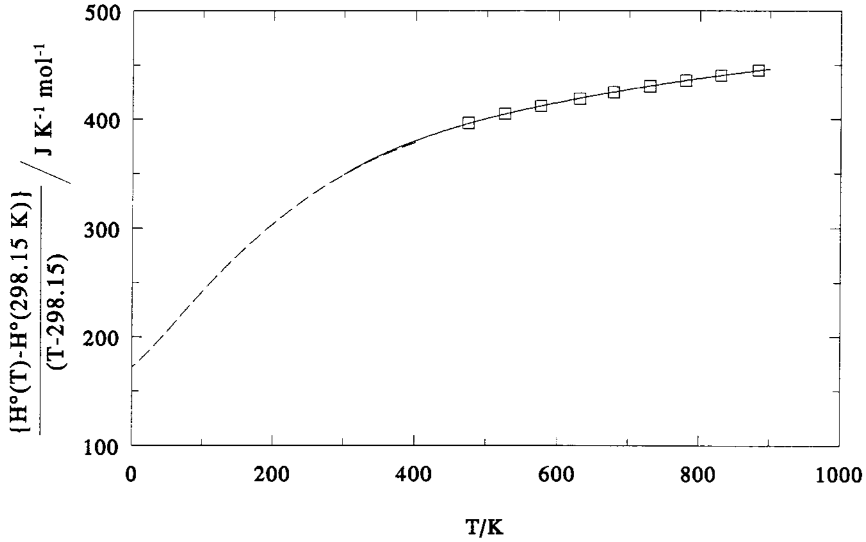

Fig. 3. The reduced enthalpy increment of YAG.

Table 2
The experimental enthalpy increments of YAG

T (K)	$\{H^0(\mathrm{T})-H^0$ (298.15 K)$\}$(J·mol^{-1})		δ (%)
	Experimental	Calculated	
473.7	69293	69451	−0.23
525.1	91713	91803	−0.10
575.7	114156	114379	−0.20
626.9	137999	137720	0.20
678.2	161275	161542	−0.17
729.0	185859	185523	0.18
780.0	210527	209959	0.27
830.3	233567	234390	−0.35
883.1	260584	260368	0.08

thermal function from 10 to 420 K. For the values of C_p^0 and S^0 at the standard reference temperature 298.15 K, we obtain:

$$S^0(298.15\,\mathrm{K}) = (284.8 \pm 0.9)\ \mathrm{J} \cdot \mathrm{K}^{-1} \cdot \mathrm{mol}^{-1}$$

$$C_p^0(298.15\,\mathrm{K}) = (348.1 \pm 0.3)\ \mathrm{J} \cdot \mathrm{K}^{-1} \cdot \mathrm{mol}^{-1}$$

The results of the drop-calorimetry measurements are listed in Table 2. The data have been fitted to the polynomial:

$$\{H^0(\mathrm{T}) - H^0(298.15\,\mathrm{K})\}/\mathrm{J} \cdot \mathrm{mol}^{-1} = 428.5233(\mathrm{T/K}) + 44.6267 \cdot 10^{-3}(\mathrm{T/K})^2 + 9.5120 \cdot 10^6(\mathrm{T/K})^{-1} - 163634.6$$

applying C_p^0 (298.15 K) = 348.13 J·K^{-1}·mol^{-1} and $\{H^0(\mathrm{T})–H^0(298.15\ \mathrm{K})\} = 0$ at 298.15 K as boundary conditions. The standard deviation of the fit is 445.9 J·mol^{-1}.

As shown in Fig. 3 in a plot of the reduced enthalpy increment, the high-temperature and low-temperature ranges fit smoothly.

The thermal functions of YAG are listed in Table 3. For the range 0 to 300 K these have been derived from the low-temperature measurements, for the 300 to 900 K from the high temperature measurements.

As stated before, there are no experimental heat capacity data are available to us to compare these results to.

Table 3
The thermodynamic functions of YAG from 0 to 900 K

T (K)	C_p^0(J·K^{-1}·mol^{-1})	S^0 (298.15 K) (J·K^{-1}·mol^{-1})	$-\{G^0(\mathrm{T})\}-H^0$ (0 K)}/T (J·K^{-1}·mol^{-1})	H^0(T)$-H^0$ (0 K)
10	0.219	0.073	0.0183	0.547
20	1.520	0.555	0.138	8.325
30	4.932	1.656	0.435	36.61
40	12.12	3.980	1.002	119.1
50	22.34	7.731	1.949	289.1
60	35.00	12.89	3.324	574.0
80	65.33	26.99	7.381	1569
100	100.0	45.18	13.06	3212
120	135.3	66.57	20.16	5569
140	168.1	89.92	28.44	8607
160	198.5	114.4	37.65	12277
180	226.5	139.4	47.56	16531
200	252.2	164.6	58.00	21321
220	275.8	189.8	68.84	26605
240	297.2	214.7	79.96	32337
260	316.5	239.3	91.27	38478
280	334.0	263.4	102.7	44986
298.15	348.1	284.8	113.2	51178
300	349.5	287.0	114.2	51823
400	404.8	396.0	171.3	89873
500	435.1	489.9	225.9	131986
600	455.7	571.1	276.8	176576
700	471.6	642.6	324.1	222965
800	485.1	706.5	368.0	270813
900	497.1	764.3	408.8	319931

References

[1] N. Cocuaud, E. Picard, R.J.M. Konings, A. Conti, Hj. Matzke, in: Proceedings GLOBAL'97, International Conference on Future Nuclear Systems, Vol. 2, Yokohama, Japan, 1997, p. 1044 (1997).

[2] R.J.M. Konings, K. Bakker, J.C. Boshoven, R. Conrad, H. Hein, J. Nucl. Mat., in press.

[3] V.A. Lysenko, G.F. Voronin, Moscow Univ. Chem. Bull. 45 (1990) 33.

[4] J.C. van Miltenburg, G.J.K. van den Berg, M.J. van Bommel, J. Chem. Thermodyn. 19 (1987) 1129.

[5] E.H.P. Cordfunke, R.P. Muis, G. Prins, J. Chem. Thermodyn. 11 (1979) 819.